Making shipping greener: ORC modelling under realistic operative conditions

Santiago Suárez de la Fuente [a*], Alistair R. Greig [a]

[a] *University College London,*
Roberts Building, Torrington Place, London, WC1E 7JE, United Kingdom

Abstract

The predictions of CO_2 atmospheric concentrations by 2050 are between 480 ppm to 550 ppm with a corresponding increase in global temperatures from 0.5 to 2.5°C. Shipping contributes 3.3% of the total human CO_2 emissions. It is therefore important to start generating green and intelligent solutions based on new strategies and technologies, which would help follow a green agenda in shipping.

The largest source of energy loss in a ship is in the propulsion system. This study focuses on the concept of managing waste heat energy from the exhaust gas. Using waste heat recovery systems to make shipping more efficient represents a good area of opportunity from an academic and industrial perspective. Organic Rankine Cycles (ORC) have been applied in land based systems before, showing improvements in performance when compared with traditional Rankine cycle. However, the use of ORC in ships has been limited, offering an important area of opportunity to be considered.

The proposed ORC waste heat recovery system was modelled with a typical slow speed diesel engine installed after the turbo compressors in the exhaust gas system. The energy recovered from the exhaust gas flow will be transformed via the thermodynamic cycle into electricity which will help to cover the ship demand. By doing this, there is a reduction in fuel consumption reduction and therefore a decrease in the emissions of CO_2 and other greenhouse gases (GHG). A code generated explicitly for this purpose compared the behaviour of different working fluids appropriate for different operative scenarios. With this it is possible to demonstrate that a simple ORC can be more effective than water based Rankine cycle, challenging previous research and common standards for the industry.

Keywords: Organic Rankine Cycle; Waste Heat Recovery Systems; ship system;

Nomenclature

Symbol	Name	Units	Symbol	Name	Units
T	Temperature	K	FS	Fuel save	g/kWh
P	Pressure	kPa	**Greek Symbol**	**Name**	**Units**
$\dot{W}$	Power	kW	ε	Ratio of mechanical power returned	-
$SFOC$	Specific Fuel Oil Consumption	g/kWh	η	Efficiency	%
$\dot{m}$	Mass flow rate	kg/s			
C_P	Specific heat	kJ/kg-K			
$\dot{Q}$	Heat transfer rate	kW			

* *Email address:* santiago.fuente.2011@ucl.ac.uk

Subscripts and superscripts	Name	Subscripts and superscripts	Name
C	Sink	o	Outlet/Out
co	Condenser	min	Minimum
c	Critical	p	Pump
e	Electrical	pp	Pinch Point
eq	equipment	r	Regenerator
ev	evaporator	$rvap$	Reduced saturated vapour point
exp	Expander	S	Sea water
gen	Generated	Sat	Saturation
H	Source	sc	Subcooler
h	High pressure	sh	Superheater
ha	Heat absorbed	t	Net
i	Inlet/In	th	Thermal
l	Low pressure	v	Vessel

1. Introduction

Total CO_2 global emissions in 2007 can be distributed according to human activity, as follows: electricity and heating 35%, transportation 27%, industry 22.8%, and the remainder in other type of energy uses (International Maritime Organization 2009). This study will focus on the shipping and fishing sector which are part of the transportation section and represent around 3.3% of the global carbon emissions (International Maritime Organization 2009).

Shipping is one of the transportation modes with the greatest growth in energy demand between the years 1990-2006. In the Organisation for Economic Co-operation and Development (OECD) countries the shipping energy demand increased by 2.0% compared to non-members where it increased by 7.3%. To give a comparison, emissions in the aviation sector in the same period grew only 3.4% and 2.1% respectively (International Energy Agency 2009). Shipping therefore represents an opportune sector to target for the reduction in CO_2 emissions.

The International Maritime Organization (IMO) predicted an average growth limit for shipping in tonne-nm† of around 147% to 302% by 2050 (International Maritime Organization 2009). These calculations are strongly linked with GDP, population, market and route growth. If no other policies are implemented and the patterns of social and economic behaviour do not change, the future CO_2 emissions in shipping will grow 400% by 2050 from the 2007 level (International Maritime Organization 2009).

Within ships, the majority of energy loses are located in the engine. From the energy obtained in the fuel's combustion process, around 30% of the energy ends as thrust, 18% is lost due to friction at the propeller and transmission losses, and the rest of the energy is found in the engine's own inefficiencies (International Maritime Organization 2009).

This energy map shows the importance of increasing the engine's thermal efficiencies in order to reduce the CO_2 emissions. The fuel energy lost in the engine can be found as heat removed from the engine by the cooling system, heat escaping from the engine surface due to convection or radiation and finally through the exhaust gases. Therefore through increasing the engine efficiency it will be possible to reduce CO_2 emissions and other GHG.

In most of the cases, diesel engines are the preferred vessel mover due to its high thermal efficiency, which can reach up to 53% (International Maritime Organization 2009). However, there is still a substantial waste energy that can be reused.

Normally the waste heat coming from the diesel exhaust gases is found as low or medium quality heat. This means that the temperature of the waste heat is between 303K to 503K for low grade heat and from 503 K to 923 K for medium grade heat (Bureau of Energy Efficiency 2004). In the case of the water cooling system, the radiative and convective heat losses are generally low grade.

Thermodynamic Waste Heat Recovery Systems (WHRS) absorb part of the waste heat which evaporates at high pressure the working fluid. Then the fluid expands in a turbine and converts part of the heat energy into mechanical, electrical or cooling work.

The use of WHRS in land based systems has been well covered using low/medium waste heat found in internal combustion engines (Dolz et al. 2012; Feng et al. 2010; Weerasinghe et al. 2010; Dinanno et al. 1983), cement processes (Cunningham 2002; Bronicki 2000) and, geothermal electric production (Street et al. 2004).

The work presented here will focus on the usage of low/medium grade waste heat energy from the exhaust gas, even though its cost of application in shipping is one of the highest (Alvik et al. 2010). However, the versatility in the uses of the waste heat gives WHRS an edge over other CO_2 reduction technologies. The waste heat can be used to generate electrical energy to cover part of the electrical demand inside the ship or for producing cooling power to assist the heating, ventilation and air conditioning (HVAC) system. The IMO predicts that by the year 2050 the WHRS could reduce CO_2 emissions by around 2-6% depending in the type of ship (Bazari & Longva 2011). Using the BIMCO EEDI calculator, MAN predicted that use of WHRS would result in a drop in the Energy Efficiency Design Index (EEDI) by around 9.2% (MAN Diesel & Turbo 2012). Using WHRS will not only mitigate CO_2, since WHRS reduces the fuel consumption, it will also reduce NO_x and other GHG emissions.

---

† The tonne-mile unit measures the activity of shipping industry. *"It is the amount of cargo shipped multiplied by the average distance that it is transported."*(International Maritime Organization 2009). This index combines demand, routes, fleet (their capacities) and growth, and can be translated to energy requirements, and finally related to CO_2 emissions. Tonne is used here as a metric ton, 1 tonne = 1,000kg. The nm stands for nautical mile, where 1nm = 1,852m.

The preferred thermodynamic WHRS used inside ships is the water based Rankine cycle (RC). There are a number of reasons which promote the use of water as a working fluid at these temperatures including (Ringler, J. et al. 2009; Chen et al. 2010; Boretti 2012):

- High critical temperature (i.e. 647 K) and high latent heat (i.e. 2,391.8 kJ/kg) which helps to deliver large power outputs at high efficiencies.
- There is no chemical deterioration or decomposition.
- At higher temperatures it can be assured that the vapour will not condense inside the turbine, eliminating the problem of erosion.

There are a number of published analyses of the performance of RC WHRS in the marine scenario. Hatchman (1991) simulated two different RC plants (single and dual pressure) inside a ship which will recover heat from a 50.5% efficient diesel engine. The objective was to observe the effects on performance at different loading scenarios (i.e. from 60% to 100% maximum continuous rating (MCR)). The RC plants were optimized to work at 583 K. The sink temperature was set to 298 K. The results of the single pressure unit show that the power output and system efficiency was directly proportional to the load. The rated MCR and source temperature of 583 K achieved a power output of 300kW$_e$ and thermal efficiency of around 6.5%, thus giving a system total plant efficiency of around 53.5%. For the double-pressure unit, the results under the same conditions yielded a power output of around 325kW$_e$, with a thermal efficiency of around 7.5% and a final total plant efficiency of around 54.5%. This is four percentage points above the diesel engine. However, these conditions are at MCR which in today's shipping behaviour are not realistic, and such WHRS power outputs and efficiencies will be achieved only for short periods of time.

WHRS for shipping based on RC have been manufactured and applied with success. Schmid (2004), presented an improved WHRS based on a dual-pressure RC. The plant used an auxiliary power turbine which helped the steam cycle and operated in a range of 55 to 100% of the MCR. The sink temperature is assumed to be 298 K. The WHRS working with a Wärtsilä engine of 68MW can improve the power output when operating at 85% MCR by 12% and with a total efficiency increase, between 49.3% to 54.9%. The approximate payback time for the investment was estimated to be 4 years. MAN (MAN Diesel & Turbo 2012) state that it is possible to increase the power output by 8 to 11% for the RC with a power turbine; from 5 to 8% with the double-pressure; and from 4 to 7% when using the single pressure RC. These power output estimates are dependent on engine load and the voyage conditions. The operability of these systems is between 50 to 100% of the MCR. The *Emma Mærsk* is powered by an 80MW diesel engine using a RC WHRS achieving a reduction of 10% in GHG emissions and a total plant efficiency of around 55% in 2006. This represents an increase from is standard efficiency of 49.3% (Hultqvist 2008). This analysis shows that the RC is a proven technology that can reduce the GHG emissions effectively by providing extra electrical power to the ship power plant.

Even though the WHRS based in the RC deliver good results, it is possible to increase the thermal efficiency and power output of a low/medium quality WHRS using organic fluids (i.e. that contain carbon in its molecular structure) instead of water. Yamamoto *et al.* (2001) found that a WHRS based on an Organic Rankine Cycle (ORC) at a source temperature of 323 K was capable of producing 12% more power output than a WHRS RC at a source temperature of 473 K.

Saavedra *et al.* (2010)compared different organic fluids to determine, after a cycle optimization, which working fluid was the best option for heat recovery from a medium grade source in order to generate electricity. In order to choose the organic working fluids Saavedra *et al.* (2010) took into account the critical temperature, critical pressure, flammability and toxicity levels of the different organic fluids. The simulations tested the WHRS at three different sink temperatures set at 308 K, 323 K and 363 K. The best ORC at a sink temperature of 308 K used Toluene and had a thermal efficiency of around 27.9% and while the RC was 24.3%. When the sink is at 323 K the ORC with ethylbenzene showed the best thermal efficiency at 25.5% and the RC delivers a thermal efficiency of 23.5%. Finally, at a temperature of 363 K the ORC with n-heptane had the best thermal efficiency at 19.5% and the RC was 16.7% (Saavedra et al. 2010).

Organic fluids have lower latent heat than water. This will translate to larger mass flow rates increasing the pump losses. However, as demonstrated before the WHRS based in the ORC can deliver better thermal efficiencies and power outputs at lower source temperature than the RC. With the increasing preference of the shipping industry for slow speed steaming, the increase of the diesel engine thermal efficiency and other GHG reduction technologies using part of the available waste heat, it is expected that the quality of the waste heat will be lower. This makes it harder for the RC to deliver

high levels of electric power at a reasonable thermal efficiency. The large catalogue of organic fluids lets the WHRS to operate at different waste heat scenarios.

In the case of ORC Opcon Marine manufactures waste heat recovery plants specially made for shipping. Its ORC plant is only made for low grade source temperature spectra (i.e. 363-433K), in particular for the cooling system's water (Opcon Energy Systems AB 2012b). The plant is capable of producing 500kW and it is coupled to the Opcon Powerbox WST, which uses the excess steam produced in a ship to reduce heat losses even further. Both waste heat recovery plants are installed in *MV Figaro* with a reported saving in fuel consumption of around 5% (Opcon Energy Systems AB 2012a), but there is no mention of the system's thermal efficiency. The operating temperatures of both equipment range between 20 to 40 K. Regarding some other examples of ORC WHRS ship applications, the literature is scarce and only a few examples were found. For example, an advertisement in the green magazine promoting a Mols-Linien ferry using an ORC power plant for waste recovery system claims it increases in ship efficiency up to 35% compared with a ferry without the system installed (Green Ships of the Future n.d.).

The literature regarding WHRS tends to find the optimum operating point of a specific scenario and from there, test how its characteristics are affected when modifying variables such as temperature or pressure. In the ship case, being a transport mode, the variables are normally changing (e.g. source and sink temperatures, waste heat mass flow rate, among others), making it difficult to find an option that will deliver a flexible system throughout the ship's full operating scope. The ship case is a peculiar one; it is different from cases like geothermal and cement plants because as it moves, its operating conditions change. However, it departs from the automotive scenario because its operating conditions normally change slowly as it covers its route. Ships operate commonly at different engine loads depending on the weather, schedule, cargo level or operational strategy, affecting the waste heat availability from the ship's different heat sources. Therefore studying this variable scenario will contribute to the understanding of WHRS in changing environments with multiple and flexible conditions. In this paper we studied how the Diesel's engine load affects the performance of the WHRS.

Based on the above, this study will help understand the advantages of the RC and ORC WHRS and their performance inside ships. The application to the shipping industry represents important challenges given the size and weight restrictions. The main goal is to determine the best thermodynamic cycle for the different ship engine operating conditions. This study presents important advantages over previous research: a) it offers an unbiased comparison of the available WHRS. This covers an important caveat on previous literature, more oriented to the research of a single cycle. b) it bridges academy and industry by offering new alternatives to increase efficiency and c) it contributes to the understanding of the application of new technologies to the reduction of CO_2 in shipping.

2. Main elements in the WHRS

2.1 Diesel engine and the exhaust gas.

The engine used is a large 14 cylinder slow speed Diesel manufactured by MAN Diesel & Turbo. The model is K98ME7.1-TII with four turbos model MAN TCA88-21. The engine works with marine Diesel oil (MDO), which has low calorific value of 42.7 MJ/kg (MAN Diesel & Turbo 2013).

The WHRS used the waste heat available from the exhaust gas after it has passed the turbo compressor process. At this point, it was assumed to have a similar behaviour to air. The exhaust gas specific heat at constant pressure was calculated as the average temperature between the temperatures at the entrance and exit of the boiler.

Since the fuel has sulphur in its composition it is expected that the exhaust gas will contain SO_x particles. Engine manufacturers recommend having a minimum temperature at the exit of the exhaust gas between 433.15 – 438.15 K to avoid soot and acid corrosion (MAN Diesel & Turbo 2009; Schmid 2004). This will mean that the WHRS boiler will be able to extract energy until the exhaust gas reaches a temperature of 433.15 K.

The engine's loading conditions considered will go from 15% to 100% of the engine's MCR. Table 1 shows the engine performance and exhaust gas characteristics at different loadings.

Table 1. Engine performance and exhaust gas behaviour at different engine loads and at ISO ambient reference conditions.

Engine Load (% MCR)	Power, $\dot{W}_t$ (kW)	Exhaust mass flow rate, $\dot{m}_H$ (kg/h)	Specific Fuel Oil Consumption, SFOC (g/kWh)	Temperature, $T_{H,i}$ (K)	Specific heat, C_{p_H}[‡] (kJ/kg-K)
100	87,200	744,300	175.5	557.15	1.028
85	74,137	687,300	171.3	518.15	1.025
75	65,415	647,700	168.6	491.15	1.022
50	43,610	465,300	169.5	501.15	1.023
25	21,805	297,500	176.1	488.15	1.022
15	13,083	212,000	184.1	468.15	1.020

2.2 Waste heat recovery system

For this study the thermodynamic cycle used a boiler, an expander with an electrical generator connected to shaft and to the ship's electrical circuit, a condenser with a sea pump in charge of the sink fluid, another pump for the working fluid and a regenerator installed after the pump and the expander. The plant layout is shown in the following figure.
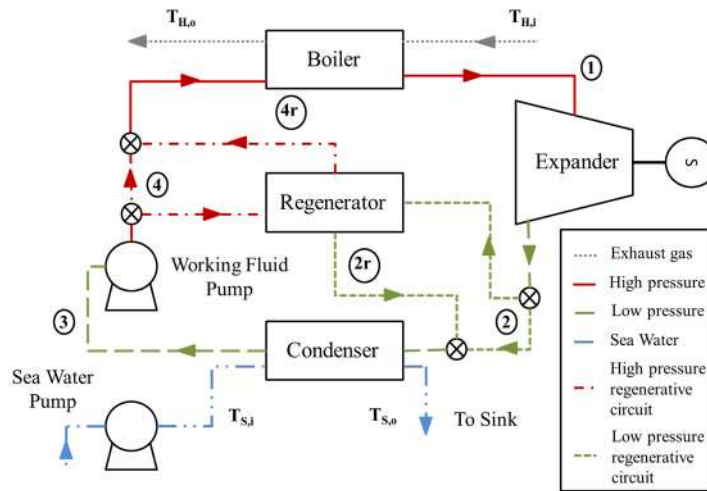

Figure 1. WHRS layout for this study.

The short dash line and point dash line represent the low and high pressure circuit for the regenerator, this will be active when T_2 is hotter than T_4, if this condition is not meet then the regenerator will be offline.

The boiler and condenser were subdivided in three regions Figure 2 in order to accurately measure the energy balance in processes where there were two states of the fluid present (i.e. liquid and vapour).
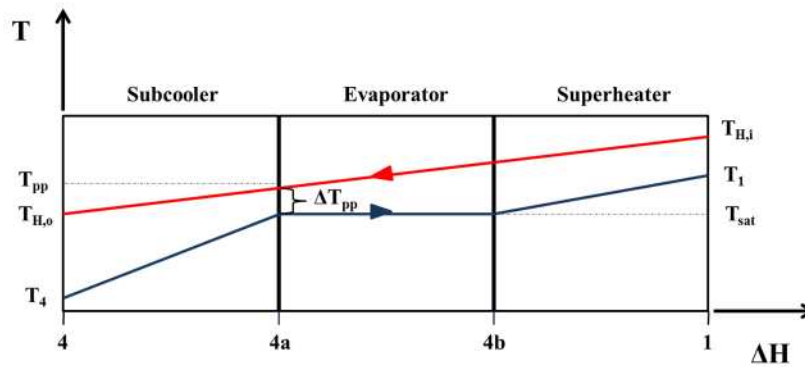

Figure 2. Representation of the three regions presented in the evaporator.

[‡] Data taken from: (Cengel & Boles 2007).

- Subcooler: In charge of the region between saturated liquid and the working fluid subcooled region. In the case of the condenser this region did not exist due to the restrictions imposed.
- Evaporator: Region that takes the working fluid from the saturated liquid state to the saturated vapour.
- Superheater: Located between the superheater state of the working fluid and the saturated vapour state.

The heat exchangers were assumed to be counter-flow and had a constant pinch point temperature difference of 5K. The pinch point temperature differences were defined as the difference between the saturation temperature and the heat source or sink temperature. As the pinch point difference was reduced, the irreversibilities of the heat transfer process were lower, but this was achieved by having larger heat exchangers.

$$T_{pp} = T_{sat} + \Delta T_{pp} \tag{1}$$

The sink pump was in charge of the sea water flow which removed the excess heat from the working fluid until it reached its liquid saturation point. The sea water was assumed to have a salinity of 35g of salt per kilogram of water and the sea pump is working at a pressure of 100kPa. The properties of the sea water were taken from Sharqawy et al. (2010).

Table 2. Operating parameters for the thermodynamic cycles.

Section of the plant layout	Variable	Value
Expander		
	Inlet temperature, T_1 (K)	$0.975 T_{H,i}$
	η_{exp}	75%
	Exit pressure, (kPa)	10
Condenser		
	$\Delta T_{pp,C}$ (K)	5
	Inlet Sink Temperature, $T_{S,i}$ (K)	293
	η_{co}	100%
Regenerator		
	η_r	90%
Pump		
	Inlet temperature, T_3 (K)	Liquid saturation temperature at low pressure
	η_p	75%
Boiler		
	$\Delta T_{pp,H}$ (K)	5
	η_{ev}	100%
	Inlet Source Temperature, $T_{H,i}$ (K)	Per Table 1
	Exit Source Temperature, T_{H,o_min} (K)	433.15

Other assumptions made for the model of the vessel's WHRS are:

- The electrical efficiency of the generator and pumps are the same and stay constant with a value of 90%.
- No pressure changes except for the expander and pump.
- No heat losses in the working fluid circuit except the ones set for the heat exchangers.
- No leakages.
- Steady-state operation.
- Only one equipment of each type is required for this study.
- Values shown in Table 2 stay constant unless the contrary is stated.

2.3 Working Fluids

The working fluids selected for this study are shown in Table 3. They were selected principally because of its good performance in the work done by Saavedra et al. (2010), the fluids are allowed to be used around the world and its availability in NIST Database software (Lemmon et al. 2010).

Table 3. Working fluids selected and some of their properties.

Working Fluids	T_c (K)	P_c (MPa)	Notes from the fluid[§]
Water	647.10	22.06	
Benzene	562.02	4.91	Highly flammable, irritating.
Toluene	591.75	4.13	Extremely flammable, irritating.
Heptane	540.13	2.74	Highly flammable, irritating, harmful to aquatic life.
Hexamethyldisiloxane (MM)	518.70	1.94	Highly flammable, irritating, harmful to aquatic life.

The critical temperature and pressure are of great importance for organic fluids, after these points are reached the fluid will start to decompose reducing its useful life in the cycle (Saavedra et al. 2010). Because of this reason the pressure and temperature limits were given by the critical points. In the case of the critical temperature if the expander inlet temperature is higher than the critical temperature of the fluid, then the inlet temperature became the critical temperature, such is the case of heptane when the engine is working at 100% MCR.

Some of the working fluids selected have a medium/high level of toxicity which require that the vessel have security systems installed and working procedures that reduce the danger of having on board the fluids selected.

3. WHRS Model

The model uses MATLAB, in particular tools from NIST Refprop (Lemmon et al. 2010) for the working fluids and the code developed by Sharqawy and Mistry (2012) for sea water properties.

The model iterated the high pressure level in steps of 10 kPa up to the critical pressure of each working fluid, in order to find the optimum operating conditions for the WHRS. The iterative process stopped when the critical pressure was reached or when the working fluid saturation temperature was higher than the value set in Table 2 for the expander inlet temperature.

3.1 Heat Exchangers

The heat flow available from the exhaust gas is defined as follows:

$$\dot{Q}_H = \dot{m}_H C_{p\_H}(T_{H,i} - T_{H,o\_min}) \tag{2}$$

With the pinch point temperature difference and the saturation temperature of the working fluid (Equation (1)) is possible to know the heat coming into the subcooler:

$$\dot{Q}_{H,sc} = \dot{m}_H C_{p\_H}(T_{sat,h} + \Delta T_{pp,H} - T_{H,o\_min}) \tag{3}$$

Equating the heat leaving the exhaust gas to the heat absorbed by the working fluid is possible to determine the mass flow rate required by the subcool region, assuming that there is no regenerator:

$$\dot{m}_{wf,sc} = \frac{\dot{m}_H C_{p\_H}(T_{sat,h} + \Delta T_{pp,H} - T_{H,o\_min})}{(h_{4a} - h_4)} \tag{4}$$

Where h_{4a} is the high pressure enthalpy at the saturated liquid point of the working fluid. $\dot{m}_{wf,sc}$ is used here as the maximum mass flow rate possible which falls inside the restrictions set by the pinch point temperature and the exhaust gas exit temperature. A lower mass flow rate than the one set by $\dot{m}_{wf,sc}$ will not be able to absorb all the energy available at the subcooler but it will still be inside the restrictions limits.

[§] Comments are written as found in the Annex VI Regulation 1272/2008 of the Institute for Health for Consumer Protection (Institute for Health for Consumer Protection 2008).

With Equations (2) and (3) is possible to determine the mass flow rate required to take the working fluid from its liquid saturated point to the expander inlet enthalpy:

$$\dot{m}_{wf,ev-sh} = \frac{\dot{Q}_H - \dot{Q}_{H,sc}}{(h_1 - h_{4a})} \qquad (5)$$

$$\dot{m}_{wf,ev-sh} \leq \dot{m}_{wf,sc} \qquad (6)$$

$\dot{m}_{wf,ev-sh}$ will be used as the working fluid mass flow rate. The logic of the code will not take into consideration mass flow rates that do not comply with the restriction shown in Equation (6). From this point onwards the $\dot{m}_{wf,ev-sh}$ will be written as $\dot{m}_{wf}$.

The total heat absorbed by the working fluid can be calculated as follows:

$$\dot{Q}_{wf,H} = \dot{Q}_{wf,H-sc} + \dot{Q}_{wf,H-ev} + \dot{Q}_{wf,H-sh} = \dot{m}_{wf}[(h_1 - h_4)] \qquad (7)$$

For the condenser the heat rejected to the sea water when there is not a regenerator is given by:

$$\dot{Q}_{wf,S} = \dot{Q}_{wf,S-sc} + \dot{Q}_{wf,S-ev} + \dot{Q}_{wf,S-sh} = \dot{m}_{wf}[(h_3 - h_2)] \qquad (8)$$

As it was explained in section 2.2, the use of the regenerator was possible if T_2 is higher than T_4. Since the regenerator was not assumed perfect the heat transfer restriction was modified to consider the regenerator efficiency:

$$T_2 > \left(1 + (1 - \eta_r)\right)T_4 \qquad (9)$$

Where η_r is given by the following equation considering constant specific heat:

$$\eta_r = \frac{T_2 - T_{2r}}{T_2 - T_4} \qquad (10)$$

And the enthalpy from the regenerator high pressure outlet is:

$$h_{4r} = (h_2 - h_{2r}) + h_4 \qquad (11)$$

3.2 Expander and pump

The power output of the expander is given by:

$$\dot{W}_o = \dot{m}_{wf}(h_1 - h_{2s})\eta_{exp} \qquad (12)$$

Where h_{2s} is the enthalpy at low pressure after an isentropic expansion.
The power input of the pump is given by:

$$\dot{W}_i = \frac{\dot{m}_{wf}(h_3 - h_{4s})}{\eta_p} \qquad (13)$$

Where h_{4s} is the enthalpy at high pressure after an isentropic compression.

3.3 Sea pump

The sea pump power input model for the Grundfos CR-150 given in kW is (Grundfos Pumps Corporation 2012):

$$\dot{W}_{S,i} = 0.1035\dot{m}_S + 13.42 \qquad (14)$$

To calculate the mass flow rate required the following equation:

$$\dot{m}_S = \frac{\dot{Q}_{wf,C}}{C_{p\_S}(T_{S,i} - T_{sat,l} + \Delta T_{pp,C})}$$ (15)

3.4 WHRS

The net power ($\dot{W}_t$) is the addition of all the power flows of the WHRS. The thermal efficiency of the WHRS is given by:

$$\eta_{th} = \frac{\dot{W}_t}{\dot{Q}_i} = \frac{\dot{W}_o + \dot{W}_i + \dot{W}_{S,i}}{\dot{m}_{wf}[(h_1 - h_4)]}$$ (16)

And the heat absorption efficiency from the boiler is as follows:

$$\eta_{ha} = \frac{\dot{Q}_i}{\dot{Q}_i} = \frac{\dot{m}_{wf}[(h_1 - h_4)]}{\dot{m}_H C_{p\_H}(T_{H,i} - T_{H,o\_min})}$$ (17)

The ratio of mechanical power returned by the WHRS to the ship is given by:

$$\varepsilon = \frac{\dot{W}_t}{\dot{W}_V}$$ (18)

Then the fuel saved by the WHRS in g/kWh is:

$$FS = \varepsilon SOFC$$ (19)

The electric power entering the ship's circuit is given by:

$$\dot{W}_e = \dot{W}_o \eta_e + \frac{(\dot{W}_i + \dot{W}_{S,i})}{\eta_e}$$ (20)

3.5 Model Validation

The code was validated against results presented by Butcher and Reddy in *"Second law analysis of a waste heat recovery based power generation system"* (Butcher & Reddy 2007) and Saavedra *et al.* in *"Thermodynamic optimization of organic Rankine cycles at several condensing temperatures: case study of waste heat recovery in a natural gas compressor station"* (Saavedra et al. 2010).

The validation process indicated that the WHRS model had an accuracy of 1.39% to the results given by Butcher and Reddy. This difference is due mainly to the fact that the mass flow rates at different pinch point temperatures were presented as graphs instead of tables, increasing the probability of a visual error by the authors. Also it was possible to detect that in their work the thermal efficiency was considering all the energy from the inlet temperature to the absolute zero temperature, which affected considerably the value thermal efficiency.

When the model is compared against the work of Saavedra *et al.* the difference was around 0.95%.

4. Results and discussion

4.1 WHRS performance at constant engine loading

In the first section the engine loading was set at 75% MCR. The thermal and heat absorption efficiency as well as power output were analysed for different working fluids and operating pressures.

Figure 3 presents how the WHRS thermal efficiency changed with respect to pressure and working fluid. Overall all the working fluids increased their thermal efficiency as the high pressure increased; this behaviour stayed up to a maximum point where the efficiency started to drop. This can

be explained by the reduction of power output from the expander with a more constant power input from the pumps. Heptane was the working fluid with the maximum thermal efficiency at 22.8% and the lower maximum thermal efficiency was set by water at 21.4%. Water produces around 52.0% less power than heptane at the maximum thermal efficiency point.
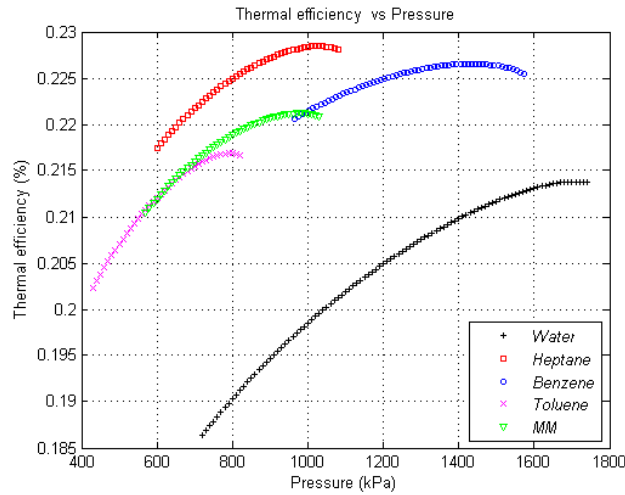

Figure 3. Thermal efficiency achieved by the working fluids at different high pressures and 75% MCR.

Table 4 shows that at the maximum thermal efficiency point benzene gave around 14.8% more power than heptane at the expense of a decrease of less than 1% of the thermal efficiency.

Table 4. Data at the maximum thermal efficiency for the different working fluids.

Working Fluids	Maximum η_{th} (%)	P (kPa)	$\dot{W}_t$ (kW)	η_{ha} (%)
Water	21.4	1,710	447	19.6
Heptane	22.8	810	932	38.3
Benzene	22.6	1,434	1,070	44.3
Toluene	21.7	1,324	721	31.2
MM	22.1	980	1,035	43.9

Figure 4 present the net power output change of the working fluids with respect to the high pressure. The maximum net power output for all the fluids is given at the lowest pressures of the iterative process. The reason is the saturation temperature and the fixed pinch point temperature difference. At low pressures, the saturation point is reached at lower temperatures allowing the working fluid to absorb more heat from the waste heat source.

Benzene is the working fluid that produces more net power and also at the highest thermal efficiency (Table 5). The before mentioned fluid is closely followed by heptane and MM. Water and heptane are the working fluids that absorb the most waste heat under the conditions set. Water rejects the most energy to the sink since it has the best heat absorption but offers the lowest thermal efficiency. This happens because the water RC, due to the low temperatures, cannot use the regenerator.

The thermal efficiencies shown in Table 5, are the highest possible when considering all the heat available in the ship's engine exhaust gas.

Table 5. Data at the maximum net power output for the different working fluids.

Working Fluids	$\dot{W}_t$ (kW)	P (kPa)	η_{th} (%)	η_{ha} (%)
Water	1,987	720	18.6	100
Heptane	2,317	600	21.7	99.9
Benzene	2,332	964	22.1	99.1
Toluene	2,142	430	20.2	99.3
MM	2,236	570	21.0	99.6

Figure 5 shows the large difference between the organic fluids and the water with respect to the mass flow rate. The reason for this is the low latent heat, which requires small amount of energy to

vaporize the working fluid, forcing larger mass flow rates to absorb the energy available (Chen et al. 2010; Maizza & Maizza 1996).

All the working fluids of this study reduced their mass flow rate as the pressure increased, caused by an increment of the pinch point temperature that rises the need of heat absorption for the subcooler region and reduces the available heat for the evaporator and superheater.

In all scenarios water had the lowest mass flow rate, which reduces the size of the equipment required such as pumps, pipes and expander. For the organic fluids, MM has the largest mass flow rate but also presented the highest drop in the mass flow rate when the pressure increases. At the maximum mass flow rate points, MM mass flow rate is more than eight times larger than water.
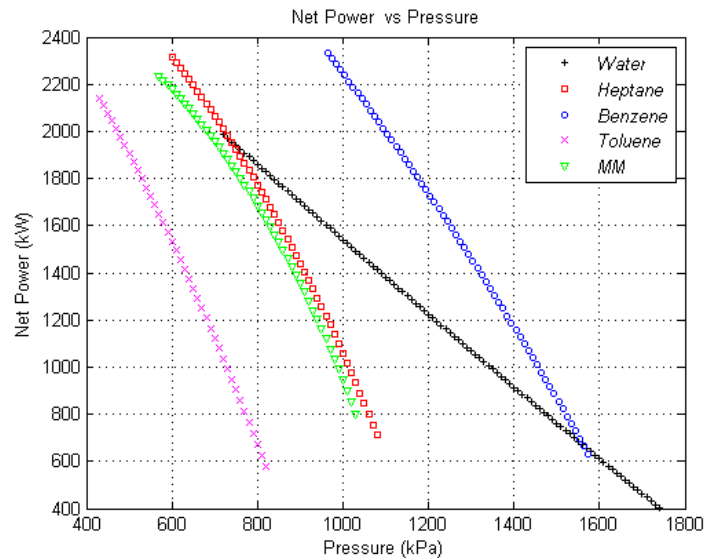
Figure 4. WHRS net power outputs at different pressures and 75% MCR.
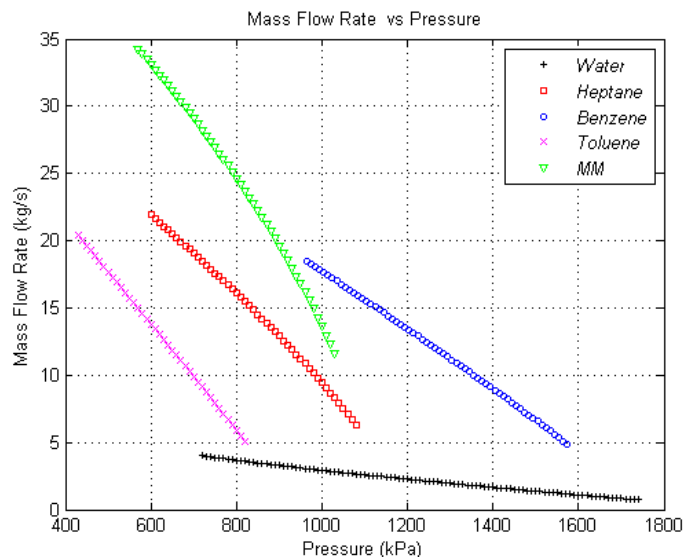
Figure 5. Mass flow rate for different working fluid and pressures.

4.2 WHRS performance at different engine loading

This section presents the results obtained when the operating conditions of the ship engine were changed, as shown in Table 1. The values are set at the maximum net power output obtained for every scenario and working fluid.

As can be seen in Figure 6, the power output increases with the engine loading. After the 75% region, a higher growth in net power output for all the working fluids is observed. There are mainly

two reasons for that: a) the exhaust mass flow rate is increasing with the engine loading deriving into more waste heat to absorb and b) the exhaust gas temperature increase due better heat transfer in the boiler.

At the low engine loading the difference between the working fluids is minimal and the net power produced is low. At the medium region, between 35% and 75%, a small difference between the organic fluids and water can be seen. For the high loading benzene, heptane and MM are the fluids that increased the most in net power output. For heptane and MM the reason was that as the saturation temperature approached the critical temperature, the energy required to take the working fluid from its saturated liquid to the energy level set by the inlet expander temperature is minimal. This allows the WHRS to increase its mass flow rate, compensating the reduction in the expander inlet enthalpy. For the case of the benzene the maximum net power was obtained from its lowest saturation temperature, which allowed the fluid to absorb large amounts of waste heat.
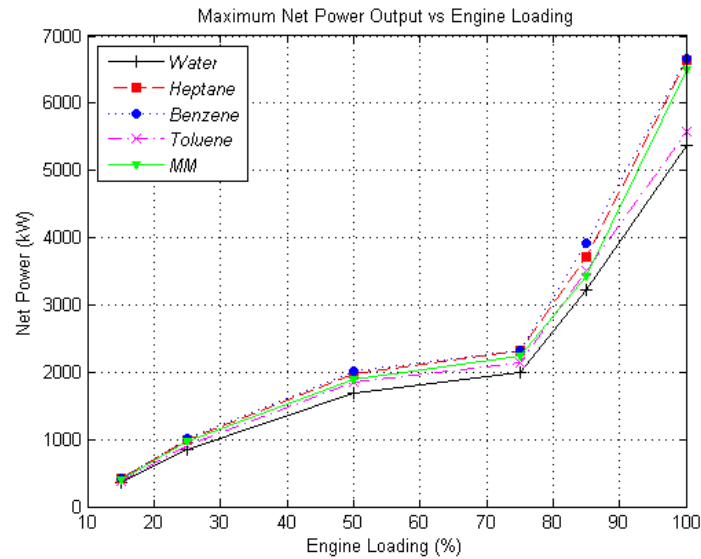

Figure 6. Maximum net power output at different engine loadings.

The maximum net electrical power behaves similarly to the net power output, caused by how Equation (20) is defined. The maximum net electric power is found at 100% MCR given by benzene at 5.9 MW_e while the lowest at the same position is water with an output of 4.8 MW_e.
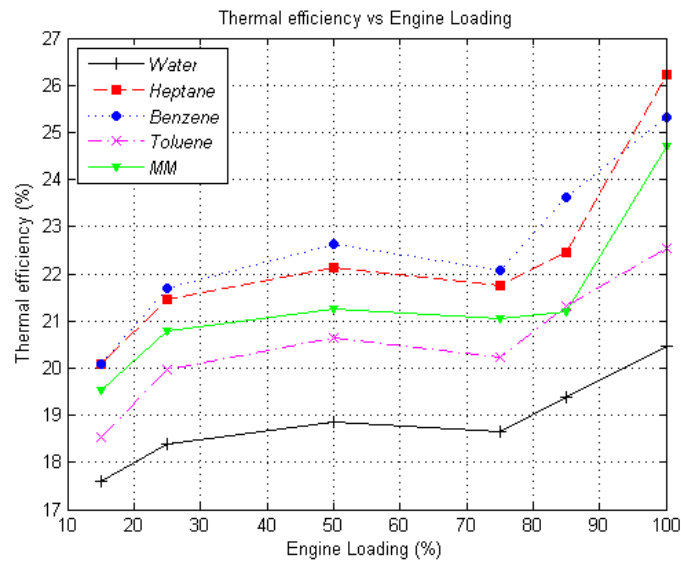

Figure 7. Thermal efficiency at the maximum net power output for different power outputs.

There are two different regions for the thermal efficiency where the working fluids behave differently. The first one goes from 15% to 75% MCR, where the thermal efficiency of all the working fluids has a peak at the 50% MCR point and after that decreases, mainly due to the exhaust heat inlet

13

temperature map. After the 75% MCR the fluid' thermal efficiency tend to increase, again this is due to the increase in the waste heat quality.

The highest thermal efficiency is given by heptane at 26.2%, and followed by benzene at 25.3%. Water's maximum thermal efficiency was the lowest of the working fluids at 20.46%.

Overall, benzene WHRS returns the largest amount of power to the ship throughout all the engine loadings, while water had the lowest participation. The biggest difference between benzene and water is reached when the engine loading is set at 100% MCR, with 1.5 percentual points of difference.
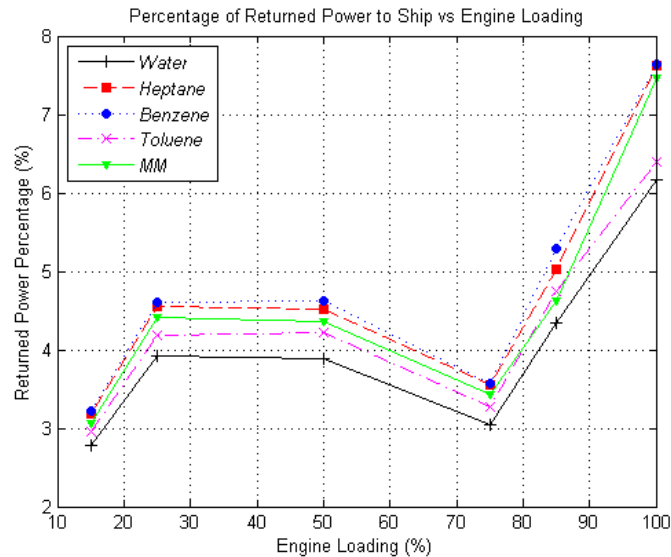

Figure 8. Percentage of power returned to the ship at different engine loading conditions.

The biggest fuel savings at low loads (i.e. below 50% MCR) at are seen at 25% MCR by benzene, which saves around 8.1g of fuel per each kWh of energy produced. The difference between benzene and water at this point is 1.2 g/kWh representing a difference of 17.6%. The highest fuel savings are seen at the 100% MCR for all fluids, where benzene and heptane return the best fuel saving at around 13.4 g/kWh, water obtained a value of 10.8 g/kWh a difference of around 23.8%.
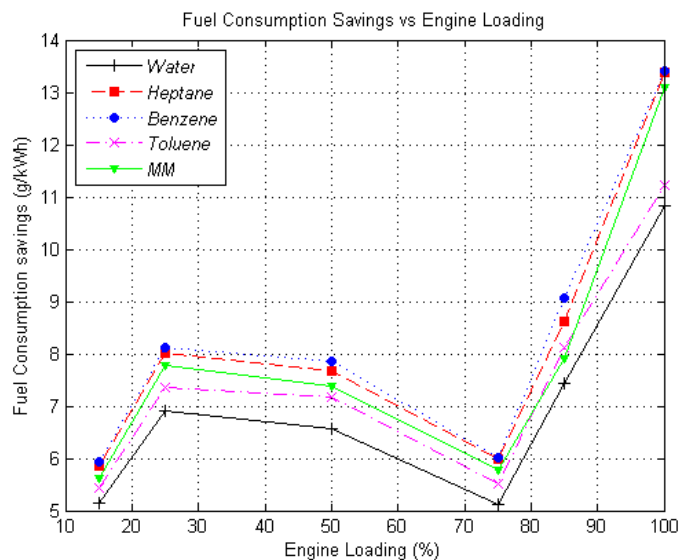

Figure 9. Fuel savings achieved by the WHRS under different operating conditions.

Figure 9 shows the advantage of using an ORC WHRS instead of a water based RC. By choosing to install an ORC WHRS not only the vessel owner will, by saving fuel, be reducing more its operating costs but also will increase the CO_2 and other GHG emissions reduction.

5. Conclusions

CO_2 emissions and other GHG have constantly increased. By reusing the energy wasted in the engine's combustion process, it is possible to contribute to mitigate the problem. WHRS represent a good area of opportunity on this regard. Previous work has mainly concentrated on land based systems or in WHRS for cars or trucks but only limited knowledge has been produced about their performance in challenging environments where size and weight are determinants, as it is the case of vessels.

By comparing the ORC and the traditional RC it is possible to offer more efficient alternatives to the shipping industry. This document adds in this direction presenting an objective and realistic comparison of the two systems.

Authors first presented results obtained modifying the high pressure level of different RC and ORC used as WHRS for the vessel's slow Diesel main engine. The pressure variation helped to visualize the behaviour of several organic fluids variables such as the WHRS net power output and thermal efficiency at a constant 75% MCR.

It was possible to distinguish the advantages of the ORC over RC WHRS: higher power output at higher thermal efficiency when using organic fluids. The working fluid that delivered the maximum net power output was benzene with 2,233 kW at a thermal efficiency of 22.1%, while water gave 1,987 kW at 18.6%. The maximum thermal efficiency seen was 22.8% achieved by heptane at a pressure of 810 kPa while the water achieved it at 21.4% with a pressure of 1,710 kPa.

The second subsection had the objective of finding how the RC and ORC WHRS behaved under different ship engine loading conditions. The points related to were the maximum found for each working fluid at the operating conditions. It was seen that the best performance of the ship's WHRS was located in the higher engine loading region, this is caused by the amount and quality of the waste heat found in the engine exhaust gas. At this region the WHRS returns large amounts of power at high thermal efficiencies, reducing the vessel's fuel consumption and CO_2 emissions.

Benzene WHRS produced a power output 23.8% larger than the water RC at a thermal efficiency of 25.3%, almost 5 percentual points more than water. The maximum fuel saving was achieved by benzene with a value of 13.4 g/kWh while water's maximum value was 10.8 g/kWh.

It can be concluded that ORC WHRS can perform better than the traditional water RC WHRS under the full range of the ship's loading conditions, meaning that using a ORC WHRS will effectively reduce the CO_2 emission and the ship's fuel need. Still it is important to consider that the large mass flow rates of an ORC WHRS will require more space inside the ship, and also there will be an installation cost increase due to the flammable and toxic characteristics of the organic fluids used in this study.

6. Future work

Future research should concentrate on:

- Create model of a marine electrical generator plant in order to quantify accurately the benefit of installing a generator to convert the expander mechanical work into electrical power.
- Add the heat transfer coefficient to the formulae of the heat exchangers, enabling the calculations for the heat exchanger size and weight.
- Find and develop, with the tools available from NIST software, organic fluids that are less toxic for humans and sea life.
- Variable expander and pump efficiencies depending on the working fluid mass flow rate.

References

Alvik, S. et al., 2010. *Pathways to low carbon shipping . Abatement potential towards 2030.*, Høvik.

Bazari, Z. & Longva, T., 2011. *Assessment of IMO Mandated Energy Efficiency Measures for International Shipping*, London.

Boretti, A. a., 2012. Transient operation of internal combustion engines with Rankine waste heat recovery systems. *Applied Thermal Engineering*, 48, pp.18–23.

Bronicki, L.Y., 2000. ORGANIC RANKINE CYCLE POWER PLANT FOR WASTE HEAT RECOVERY. , p.6.

Bureau of Energy Efficiency, 2004. 8 . WASTE HEAT RECOVERY. *The National Certification Examination for Energy Managers and Energy Auditors*, pp.1–18. Available at: http://www.em-ea.org/Guide Books/book-2/2.8 Waste Heat Recovery.pdf [Accessed April 27, 2012].

Butcher, C.J. & Reddy, B.V., 2007. Second law analysis of a waste heat recovery based power generation system. *International Journal of Heat and Mass Transfer*, 50(11-12), pp.2355–2363.

Cengel, Y.A. & Boles, M.A., 2007. *Thermodynamics: An Engineering Approach* 6th ed., Singapore: McGraw-Hill.

Chen, H., Goswami, D.Y. & Stefanakos, E.K., 2010. A review of thermodynamic cycles and working fluids for the conversion of low-grade heat. *Renewable and Sustainable Energy Reviews*, 14(9), pp.3059–3067.

Cunningham, P., 2002. Waste Heat/Cogen Opportunities in the Cement Industry. *Cogeneration & Distributed Generation Journal*, 17(3), pp.31–51.

Dinanno, L.R., Dibella, F.A. & Koplow, M.D., 1983. *An RC-1 Organic Rankine Bottoming Cycle for an Adiabatic Diesel Engine*, Cleveland.

Dolz, V. et al., 2012. HD Diesel engine equipped with a bottoming Rankine cycle as a waste heat recovery system. Part 1: Study and analysis of the waste heat energy. *Applied Thermal Engineering*, 36, pp.269–278.

Feng, L. et al., 2010. Heat Recovery from Internal Combustion Engine with Rankine Cycle. In *2010 Asia-Pacific Power and Energy Engineering Conference*. Chengdu: IEEE, pp. 1–4.

Green Ships of the Future, Green Ship Magazine. , p.32.

Grundfos Pumps Corporation, 2012. Grundfos Product Guide: CR, CRI, CRN, CRE, CRIE, CRNE - Vertical multistage centrifugal pumps. , p.89.

H., M., Sharqawy & Mistry, K.H., 2012. Thermophysical properties of seawater.

Hatchman, J.C., 1991. Steam cycles for waste heat recovery: A case study. *R&D Journal*, 7(3), pp.32–38.

Hultqvist, A., 2008. Measures for reducing emissions on Emma Maersk. , (January), p.43.

Institute for Health for Consumer Protection, 2008. Annex VI to Regulation (EC) No 1272/2008 on Classification, Labelling and Packaging of Dangerous Substances. *Annex VI to Regulation (EC) No 1272/2008*, p.1.

International Energy Agency, 2009. *Transport, Energy and CO2*, Paris: International Energy Agency (IEA).

International Maritime Organization, 2009. *MEPC 59/Inf. 10*,

Lemmon, E.W.., Huber, M.L.. & McLinden, M.O.., 2010. NIST Reference Fluid Thermodynamic and Transport Properties Database.

Maizza, V. & Maizza, A., 1996. Working fluids in non-steady flows for waste energy recovery systems. *Applied Thermal Engineering*, 16(7), pp.579–590.

MAN Diesel & Turbo, 2013. Engine room and performance data for 14K98ME7.1-TII with 4 x MAN TCA88-21 and part load exhaust gas bypass (EGB) tuning. , p.10.

MAN Diesel & Turbo, 2009. *Soot Deposits and Fires in Exhaust gas Boilers*, Copenhagen.

MAN Diesel & Turbo, 2012. *Waste Heat Recovery System (WHRS) for Reduction of Fuel Consumption, Emission and EEDI*, Copenhagen.

Opcon Energy Systems AB, 2012a. Commissioning and testing of first reference installation of Opcon technology for ships. , p.2.

Opcon Energy Systems AB, 2012b. Data Sheet OPB-ORC-750M. , p.11.

Ringler, J. et al., 2009. Rankine Cycle for Waste Heat Recovery of IC Engines. *SAE Int. J. Engines*, 1(2), pp.67–76.

Saavedra, I., Bruno, J.C. & Coronas, A., 2010. Thermodynamic optimization of organic Rankine cycles at several condensing temperatures: case study of waste heat recovery in a natural gas compressor station. *Proceedings of the Institution of Mechanical Engineers, Part A: Journal of Power and Energy*, 224(7), pp.917–930.

Schmid, H., 2004. WASTE HEAT RECOVERY (WHR): FUEL SAVINGS WITH LESS EMISSIONS. In *Green Ship Technology Conference*. London, p. 10.

Sharqawy, M.H., Lienhard V, J.H. & Zubair, S.M., 2010. Thermophysical properties of seawater: A review of existing correlations and data. *Desalination and Water Treatment*, 16, pp.354–380.

Street, E., Ny, N.Y. & Mlcak, H.A., 2004. An Introduction to the Kalina Cycle. In G. E. Kielasa, L.; Weed, ed. *The International Joint Power Generation Conference*. New York: ASME International, pp. 1–11.

Weerasinghe, W.M.S.R., Stobart, R.K. & Hounsham, S.M., 2010. Thermal efficiency improvement in high output diesel engines a comparison of a Rankine cycle with turbo-compounding. *Applied Thermal Engineering*, 30(14-15), pp.2253–2256.